A search for interstellar gas-phase CO$_2$[*]

Gas: solid state abundance ratios

E.F. van Dishoeck[1], **F.P. Helmich**[1], **Th. de Graauw**[2,4], **J.H. Black**[3], **A.C.A. Boogert**[4], **P. Ehrenfreund**[1], **P.A. Gerakines**[5], **J.H. Lacy**[6], **T.J. Millar**[7], **W.A. Schutte**[1], **A.G.G.M. Tielens**[8], **D.C.B. Whittet**[5], **D.R. Boxhoorn**[2,9], **D.J.M. Kester**[2], **K. Leech**[9], **P.R. Roelfsema**[2,9], **A. Salama**[9], and **B. Vandenbussche**[9,10]

[1] Leiden Observatory, P.O. Box 9513, 2300 RA Leiden, The Netherlands
[2] SRON, P.O. Box 800, 9700 AV Groningen, The Netherlands
[3] Onsala Space Observatory, Chalmers University of Technology, S-43992 Onsala, Sweden
[4] Kapteyn Astronomical Institute, P.O. Box 800, 9700 AV Groningen, The Netherlands
[5] Department of Physics, Applied Physics & Astronomy, Rensselaer Polytechnic Institute, Troy, NY 12180, USA
[6] Department of Astronomy, University of Texas at Austin, Austin, TX 78712-1083, USA
[7] Department of Physics, UMIST, P.O. Box 88, Manchester M60 1QD, UK
[8] NASA-Ames Research Center, MS 245-3, Moffett Field, CA 94035, USA
[9] ISO Science Operation Center, Astrophysics Dvision of ESA, P.O. Box 50727, E-28080 Villafranca/Madrid, Spain
[10] Instituut voor Sterrenkunde, K.U. Leuven, Celestijnenlaan 200B, B-3001 Heverlee, Belgium

Abstract. We present searches for gas–phase CO$_2$ features in the ISO–SWS infrared spectra of four deeply embedded massive young stars, which all show strong solid CO$_2$ absorption. The abundance of gas–phase CO$_2$ is at most $2. \, 10^{-7}$ with respect to H$_2$, and is less than 5% of that in the solid phase. This is in strong contrast to CO, which is a factor of 10–100 more abundant in the gas than in solid form in these objects. The gas/solid state ratios of CO$_2$, CO and H$_2$O are discussed in terms of the physical and chemical state of the clouds.

Key words: ISM: abundances; ISM: molecules; ISM: individual: AFGL 2591, AFGL 4176, AFGL 2136, NGC 7538 IRS9

1. Introduction

Although more than 100 different molecules have been identified in the interstellar gas, some of the simplest species have remained elusive. Either their presence in the Earth's atmosphere has blocked astronomical observations, or they have no strong millimeter transitions because of their symmetry. CO$_2$ suffers from both problems, so that up to now only indirect searches of the chemically related HOCO$^+$ ion have been possible from

the ground (Thaddeus et al. 1981; Minh et al. 1988, 1991). The *Short Wavelength Spectrometer* (SWS) (de Graauw et al. 1996a) on board the *Infrared Space Observatory* (ISO) (Kessler et al. 1996) opens up the possibility to search for the infrared–active asymmetric stretch and bending modes of gas–phase CO$_2$ around 4.3 and 15.0 μm along the line of sight toward bright infrared sources.

CO$_2$ is predicted to be one of the more abundant carbon– and oxygen–bearing molecules in the gas phase (e.g., Herbst & Leung 1989; Millar et al. 1991), and as such forms a significant test case of the chemical networks. Moreover, the detection of abundant solid CO$_2$ in interstellar clouds by d'Hendecourt & de Muizon (1989) and de Graauw et al. (1996b) suggests that CO$_2$ could be a particularly sensitive probe of gas–grain interactions. The observed abundance of solid CO$_2$ with respect to hydrogen of about $\sim (1-5) \, 10^{-6}$ is a factor of 10 larger than that predicted by cold gas–phase models. Thus, large amounts of gas–phase CO$_2$ could be produced by the evaporation or destruction of icy grain mantles. Comparison of the observed gas/solid CO$_2$ ratios with those of other species known to be abundant in icy mantles, especially H$_2$O and CO, will allow us to address the formation route of CO$_2$.

We present here searches for gas–phase CO$_2$ in the spectra of four deeply embedded young stellar objects. Mitchell et al. (1989, 1990) have measured near–infrared absorption lines of gas–phase ^{12}CO and ^{13}CO for three of these objects (GL 2591, GL 2136, NGC 7538 IRS9) at high spectral resolution from the ground, which indicate the presence of both cold, $T_{\rm kin} = 15 - 60$ K, and warm, $T_{\rm kin} = 120 - 1000$ K, gas along the lines of

sight. We use these data, together with the new ISO data on solid CO_2 of de Graauw et al. (1996b) and on gaseous H_2O by van Dishoeck & Helmich (1996), to constrain the gas/solid abundance ratios for these objects.

2. Search for gas–phase CO_2

We searched for gas–phase CO_2 in the ISO–SWS spectra through its fundamental ro–vibrational ν_3 and ν_2 transitions at 4.257 and 14.984 μm, respectively. The observational data are the same as those used by de Graauw et al. (1996b) to investigate solid CO_2, and were taken with AOT06. At 15 μm, systematic instrumental noise was removed with a Fourier transform method.

Gas–phase molecules can be distinguished from solid state features at the resolving power $\lambda/\Delta\lambda \approx 2000$ of the SWS grating by their characteristic ro–vibrational structure. This is clearly illustrated in Figure 1, which contains the 4.1-4.7 μm spectrum of GL 2591. It shows the complete R–branch and part of the P–branch of the $v = 1 - 0$ band of gas–phase CO centered at 4.67 μm, together with the strong, broad single absorption feature due to solid CO_2. The lack of individual P– and R–lines due to gas–phase CO_2, together with the absence of any broad absorption feature due to solid CO, indicates a very different chemical behavior for the two species: most of the CO is in the gas phase, whereas most of the CO_2 is in solid form.

2.1. ν_3 band

In order to constrain the amount of gas–phase CO_2, simulated spectra have been made following the method of Helmich (1996). The frequencies and intensities of the lines in the ν_3 $\Sigma - \Sigma$ asymmetric stretch were taken from the HITRAN data base (Rothman et al. 1992a; see also Rothman et al. 1992b for the molecular parameters). All levels up $J'' = 90$ (corresponding to 4585 K above ground) were taken into account in the model. CO_2 is a symmetric molecule with zero nuclear spin so that all odd–numbered rotational levels are missing. The adopted Doppler parameters b and excitation temperatures are based on infrared absorption line observations of warm gaseous CO (Mitchell et al. 1990) (see Table 1). The CO_2 rotational excitation can also be affected by pumping by infrared radiation at 15 μm, but is likely to be thermalized at densities of $10^3 - 10^5$ cm^{-3} except in regions where the temperature characterizing the radiation field at 15 μm exceeds 75 K.

Figure 1 includes a simulated spectrum of gas–phase CO_2 for a column density of 5. 10^{16} cm^{-2}, b=7.5 km s^{-1}, and $T_{\rm ex}$=250 K. The position of the gas–phase CO_2 ν_3 stretch is not shifted significantly from that of solid CO_2, so that the P– and R–branch structure will be superposed on the solid feature. Since such structure is not seen, 5. 10^{16} cm^{-2} is the maximum column density that could be hidden under the solid CO_2 feature. The inferred limit on the gas–phase CO_2 changes by at most a factor of 2 if b is varied from 5 to 12 km s^{-1} and $T_{\rm ex}$ from 100 to 500 K. No useful limits can be obtained on the amount of CO_2 in cold gas with small b-values (< 2 km s^{-1}) from the ν_3-band data.
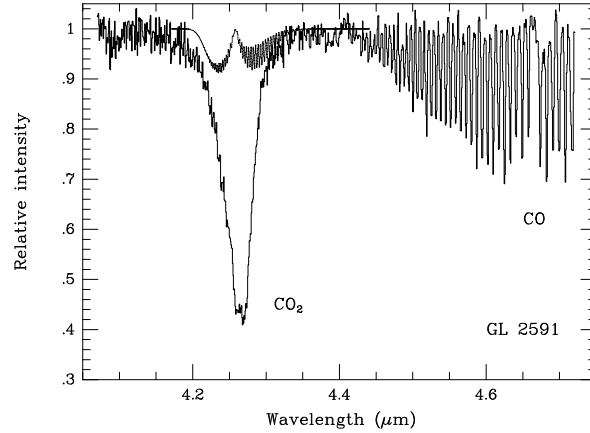
Fig. 1. ISO–SWS grating spectrum toward the embedded young stellar object GL 2591 in the 4.1–4.7 μm region. Broad absorption due to solid CO_2 is seen at 4.26 μm, as well as a forest of R– and P–branch lines between 4.4 and 4.7 μm due to warm, gas–phase CO. The light (dotted) line indicates the model absorption spectrum of gas–phase CO_2 using a column density of 5. 10^{16} cm^{-2}, b=7.5 km s^{-1} and $T_{\rm ex}$=250 K.

Similar limits are obtained toward GL 4176 and GL 2136 (see Table 1). The ν_3 solid CO_2 feature toward NGC 7538 IRS9 is so strong and broad (see de Graauw et al. 1996b) that no useful limits can be obtained.

2.2. ν_2 band

More stringent constraints on the gas–phase CO_2 can be deduced from the ν_2 bending mode data. This transition is of $\Pi - \Sigma$ type and has a Q–branch in addition to the P– and R–branch lines. Because all Q–branch lines coalesce into a single feature at the resolving power of the ISO–SWS grating, the Q–branch produces stronger absorption, even though the ν_2 band is intrinsically a factor of 10 weaker than the ν_3 band. Moreover, the gas–phase ν_2 band is shifted by at least 0.2 μm to the blue compared with the solid CO_2 bending mode, and can therefore be more easily detected on the shoulder of the solid state feature. Finally, the continuum is stronger at 15 μm than at 4 μm in these objects, so that higher S/N can be achieved.

Figure 2 shows the ISO–SWS spectra of the four sources around 15 μm, with model CO_2 spectra included. The line frequencies have been calculated using the constants of Paso et al. (1980), whereas the band strength of Reichle & Young (1972) is adopted. These values agree well with those given in HITRAN. Two cases are considered. First, the same b–values and high excitation temperatures as for the ν_3 model spectra have been used. The resulting spectra for $N(CO_2)$=1. 10^{16} cm^{-2} are shown in Figure 2 for GL 2591 and GL 4176. Second, limits on the CO_2 in the cold, quiescent gas have been studied. For GL 2136 and NGC 7538 IRS9, $T_{\rm ex}$=25 K and b=1.5 km s^{-1} are adopted. As Table 1 and Figure 2 show, the ν_2 band data are equally sensitive to the warm and the cold gas.

It is seen that in all four sources, a 3–4σ absorption feature is present at the position of the CO_2 ν_2 Q–branch. The corresponding CO_2 column densities are comfortably below the up-

Table 1. Inferred gas–phase CO_2 column densities and abundances

Object	ν_3 band cm^{-2}	ν_2 band^a cm^{-2}	$x(CO_2)^a$	T_{ex} K	b km s^{-1}
N7538 I9	...	$8.\,10^{15}$	$1.6\,10^{-7}$	200	5.0
	...	$8.\,10^{15}$	$1.6\,10^{-7}$	25	1.5
GL 2136	$< 5.\,10^{16}$	$1.\,10^{16}$	$9.0\,10^{-8}$	250	5.0
	...	$1.\,10^{16}$	$9.0\,10^{-8}$	25	1.5
GL 2591	$< 5.\,10^{16}$	$1.\,10^{16}$	$1.0\,10^{-7}$	250	7.5
GL 4176	$< 2.\,10^{16}$	$5.\,10^{15}$	$6.7\,10^{-8}$	250	5.0

^{a} Tentative values

per limits derived from the ν_3 band data. The Q–branch data are highly suggestive of the presence of gas–phase CO_2, especially toward GL 2136 and NGC 7538 IRS9. The major problem with the identification is the limited S/N of the data. The presence of gas–phase CO_2 could be confirmed through high S/N, high resolution Fabry–Perot data. The feasibility of such observations is currently uncertain, but until better data are obtained the column densities listed in Table 1 should be regarded as tentative.

2.3. Gas–phase CO_2 abundance

The column densities of $\sim 10^{16}$ cm^{-2} derived above correspond to gas–phase CO_2 abundances with respect to total H_2 of $\sim 10^{-7}$ (see van Dishoeck & Helmich 1996 for the adopted H_2 column densities). These abundances are more than an order of magnitude smaller than the limits of $< 2.\,10^{-6}$ (or $CO_2/CO<0.01$) derived from HOCO$^+$ by Minh et al. (1988) for several clouds, including NGC 7538. HOCO$^+$ has been detected in Galactic Center clouds, with an inferred CO_2 abundance of $\sim 10^{-5}$.

Pure gas–phase models predict steady–state CO_2 abundances of $3.6\,10^{-7}$ (Millar et al. 1991) and $(1.3 - 4.4)\,10^{-7}$ (Herbst & Leung 1989) using dark cloud parameters. At higher temperatures, $\sim 7.\,10^{-7}$ is found (Helmich 1996). Thus, the observed CO_2 abundances are even lower than expected from pure gas–phase chemistry. The primary production route is through $CO + OH \rightarrow CO_2 + H$, whereas destruction in cold clouds occurs by cosmic ray induced photons, and reactions with ions such as H_3^+, H^+, He^+, C^+ and N_2H^+.

3. Gas/solid state abundance ratios

The derived column densities of gas–phase CO_2 of at most 10^{16} cm^{-2} are significantly lower than the observed column densities of solid CO_2 of $10^{17} - 10^{18}$ cm^{-2} for the same lines of sight (de Graauw et al. 1996b). Thus, typically less than 5% of the CO_2 is in the gas phase. This is in strong contrast with CO and H_2O. Table 2 lists the gas/solid state abundance ratios for the three species for the four sources. It is seen that in all four sources, CO is principally in the gas phase, whereas the gas/solid state H_2O ratio varies from less than 4% for NGC 7539 IRS9 to unity for GL 2591 and GL 4176.

It is tempting to ascribe the latter variation to an increase in the amount of high temperature gas and dust. The CO data of Mitchell et al. indicate that less than 2% of the gas is at $T_{kin} >100$

Table 2. Gas/solid state abundance ratios^a

Object	CO	CO_2	H_2O
NGC 7538 IRS9	10	0.01	<0.04
GL 2136	200	0.02	0.4
GL 2591	>400	0.04	1.1
GL 4176	>400	0.04	2.2

^{a} Based on gas–phase CO from Mitchell et al. (1990), solid CO from Tielens et al. (1991) and Ehrenfreund et al. (1996, in preparation, GL 4176), solid CO_2 and solid H_2O from de Graauw et al. (1996b), and gas–phase H_2O from Helmich et al. (1996) and van Dishoeck & Helmich (1996)

K in NGC 7538 IRS9, whereas this fraction is 50-70% for GL 2591 and GL 2136. The H_2O icy mantles start to evaporate when the dust temperature is 90 K or higher. Alternatively, shocks associated with the outflows could have removed the ice mantles and created high–temperature conditions in which H_2O is rapidly produced through neutral–neutral gas–phase reactions. All three sources are known to have massive outflows, but in GL 2591 and GL 2136 the outflows have apparently affected a larger volume of the surrounding cloud than in NGC 7538 IRS9. If this is an evolutionary effect, it would indicate that NGC 7538 IRS9 is at an earlier state than the other two sources. Less information is available for GL 4176, but the fact that it has the smallest abundance of solid CO_2 and H_2O of the sources studied here and no solid CO absorption suggests a large fraction of high temperature gas.

The large fraction of CO in the gas phase is not surprising, because solid CO readily evaporates at dust temperatures above 20 K. The real mystery is why the gas to solid ratio of H_2O is so much larger than that of CO_2 in three of the sources. If evaporation of icy mantles were the main production mechanism, the CO_2 gas/solid state ratio would be expected to be comparable to or larger than that of H_2O, because its sublimation temperature of $\sim$45-72 K is lower than that of H_2O (Sandford & Allamandola 1990).

There are at least four possible explanations for this dilemma. The first, unlikely possibility is that solid CO_2 is trapped in a matrix or clathrate which only allows evaporation at much higher temperatures than H_2O. Second, one can speculate that, perhaps due to the chemistry involved, solid CO_2 is characteristic for ices in dark clouds and not for (high density) regions which collapse and form stars. In that case, CO_2–containing ices may never be heated to the sublimation temperature of CO_2.

Third, CO_2 could be destroyed on short time scales ($< 10^4$ yr) in the hot, dense gas following evaporation. Most reactions of CO_2 with abundant species (H, O, N, C, ...) have huge activation energies. However, there are some species for which the rates are larger. For example, Si atoms react with CO_2 to form SiO and CO with a rate coefficient of $1.1\,10^{-11}$ cm^3 s^{-1} at 300 K (Husain & Norris 1978). This could be an effective destruction path if Si atoms were present with an abundance of 10^{-7} or more. Alternatively, CO_2 could be effectively destroyed in the vibrationally excited state.
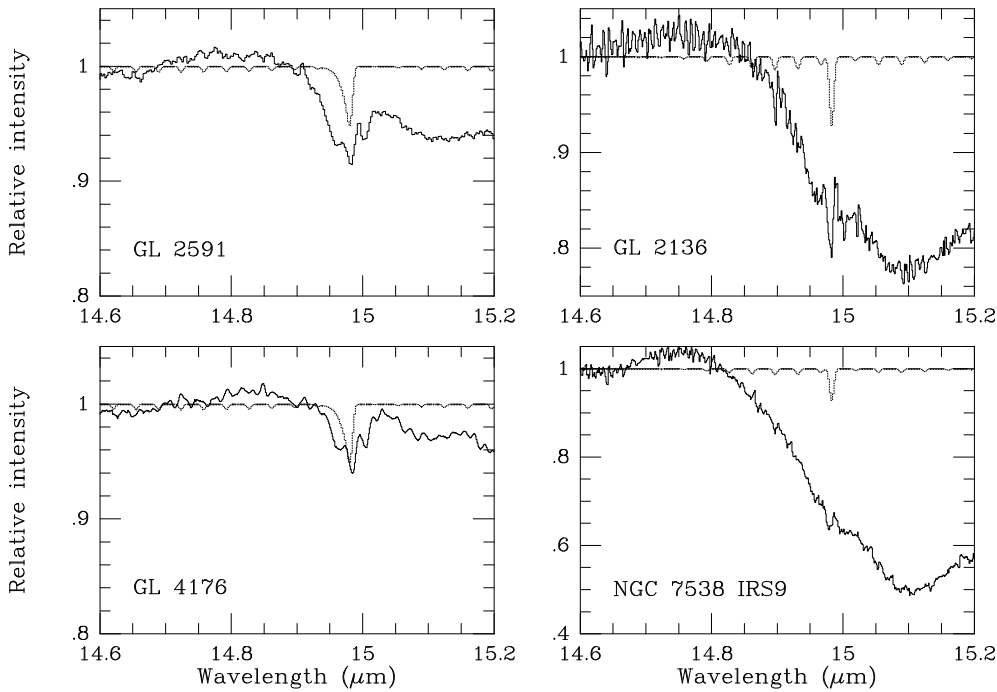
Fig. 2. Normalized ISO–SWS grating spectra toward four embedded young stellar objects around 15μm. The broad absorption feature starting around 14.8 μm is due to solid CO$_2$. The light (dotted) lines indicate the model absorption spectra of gas–phase CO$_2$ for N(CO$_2$)=1. 10^{16} cm^{-2}. For GL 2591 and GL 4176, the same b and T_{ex} as for the ν_3 band are used. For GL 2136 and NGC 7538 IRS9, b=1.5 km s^{-1} and T_{ex}=25 K are adopted, resulting in a narrower Q–branch feature.

The final, perhaps most plausible explanation is that a large fraction of the observed gas–phase H$_2$O does not originate from icy mantles but from high–temperature gas–phase reactions in shocks or radiatively heated gas. This scenario can be tested by observations once a larger data set is available (van Dishoeck & Helmich 1996). Also, comparison with the gas/solid state ratios of other species such as CH$_4$, C$_2$H$_2$ and HCN, which are not readily produced by high temperature reactions, should provide insight (Carr et al. 1995, Boogert et al. 1996). Observations of the HDO/H$_2$O ratio could test this scenario as well.

In summary, the ISO–SWS observations demonstrate that gas–phase CO$_2$ is not abundant in interstellar clouds, in spite of the ubiquitous presence of solid CO$_2$. Further searches for gas–phase CO$_2$ and other species in a larger variety of sources are warranted to test the different explanations. This study also demonstrates the potential of ISO to obtain reliable gas to solid state abundance ratios, which should provide insight into the physical and chemical evolution during star formation.

References

Boogert, A.C.A., et al. 1996, this volume

Carr, J., Evans, N.J., Lacy, J.H., Zhou, S. 1995, ApJ 450, 667

de Graauw, Th., et al. 1996a, this volume

de Graauw, Th., et al., 1996b, this volume

d'Hendecourt, L., Jourdain de Muizon, M. 1989, A&A 223, L5

Helmich, F.P., 1996, PhD thesis, University of Leiden

Helmich, F.P., et al. 1996, this volume

Herbst, E., Leung, C.M., 1989, ApJS 69, 271

Husain, D., Norris, P.E., 1978, J. Chem. Soc. Far. Trans. 74, 106

Kessler, M.F. et al. 1996, this volume

Millar, T.J., Rawlings, J.M.C., Bennett, A., Brown, P.D., Charnley, S.B., 1991, A&AS 87, 585

Minh, Y.C., Irvine, W.M., Ziurys, L.M., 1988, ApJ 334, 175

Minh, Y.C., Brewer, M.K., Irvine, W.M., Friberg, P., Johansson, L.E.B., 1991, A&A 244, 470

Mitchell, G.F., Curry, C., Maillard, J.–P., Allen, M., 1989, ApJ 341, 1020

Mitchell, G.F., Maillard, J.–P., Allen, M. 1990, ApJ 363, 554

Paso, R., Kauppinen, J., Antilla, R., 1980, J. Mol. Spectrosc. 79, 236

Reichle, H.G., Young, C., 1972, Can. J. Phys. 50, 2662

Rothman, L.S., Gamache, R.R., Tipping, R.H. et al., 1992a, J. Quant. Spectrosc. Radiat. Transfer 48, 469

Rothman, L.S., Hawkins, R.L., Wattson, R.B., Gamache, R.R., 1992b, J. Quant. Spectrosc. Radiat. Transfer 48, 537

Sandford, S.A., Allamandola, L.J., 1990, ApJ 355, 357

Thaddeus, P., Guelin, M., Linke, R.A. 1981, ApJ 246, L41

Tielens, A.G.G.M., Tokunaga, A.T., Geballe, T.R., Baas, F., 1991, ApJ 381, 181

van Dishoeck, E.F., Helmich, F.P., 1996, this volume